ARTICLES
https://doi.org/10.1038/s41593-018-0136-y
nature neuroscience

Encoding of error and learning to correct that error by the Purkinje cells of the cerebellum

David J. Herzfeld[1,2*], Yoshiko Kojima[3], Robijanto Soetedjo[3] and Reza Shadmehr[1]

The primary output cells of the cerebellar cortex, Purkinje cells, make kinematic predictions about ongoing movements via high-frequency simple spikes, but receive sensory error information about that movement via low-frequency complex spikes (CS). How is the vector space of sensory errors encoded by this low-frequency signal? Here we measured Purkinje cell activity in the oculomotor vermis of animals during saccades, then followed the chain of events from experience of visual error, generation of CS, modulation of simple spikes, and ultimately change in motor output. We found that while error direction affected the probability of CS, error magnitude altered its temporal distribution. Production of CS changed the simple spikes on the next trial, but regardless of the actual visual error, this change biased the movement only along a vector that was parallel to the Purkinje cell's preferred error. From these results, we inferred the anatomy of a sensory-to-motor adaptive controller that transformed visual error vectors into motor-corrections.

Cerebellar Purkinje cells (P-cells) produce high frequency simple spikes (SS) to predict kinematics of the ongoing movement[1–6]. These SSs are adaptable, changing following experience of a sensory error[7–9], which are transmitted to P-cells from the inferior olive[10], resulting in complex spikes (CS)[11–13]. However, CSs are rare events that occur approximately once per second[14], producing a disparity between richness of information regarding predictions via the SSs and the poverty of sensory error information in the CSs. Indeed, errors can double[15,16] or halve in size[17] without significant changes in CS rates. How can P-cells accurately produce SSs when their teacher is seemingly so impoverished in its encoding of sensory errors?

One possibility is that error magnitude modulates the shape of CS waveforms. Properties of a sensory stimulus can affect the number of spikes in the climbing fiber[18], thereby altering the duration of the resulting CS waveform[19,20]. A longer CS waveform has been shown to induce a larger change in the SSs, producing a larger change in behavior[21,22].

Another possibility is that error magnitude may affect CS timing. The latency of the CS with respect to SSs in the flocculus has been shown to modulate plasticity at the parallel fiber to P-cell synapse[23]. That is, CSs that arrive during a precise temporal window may have a larger effect on the SSs by maximizing the change in the strength of the recently active P-cell synapses.

Here we considered saccadic eye movements to visual targets. At saccade end, sometimes the subject's gaze missed the target, resulting in an error. We quantified how CSs encoded the vector space of visual errors, how this encoding changed the SSs that were produced in the subsequent saccade, and how the motor output in this subsequent saccade differed from those that the animal had produced before the experience of error.

We found that in the oculomotor vermis, each P-cell had a preference for a specific direction of visual error[16,24], with the error direction encoded in the probability of generating a CS. However, the magnitude of that error vector affected CS timing. As the error became larger, CS timing became less variable and more likely to occur during a specific temporal window: the window that was most effective in inducing plasticity. Notably, CSs that occurred in this temporal window had a longer waveform duration. Using trial-by-trial analysis[7,9,21], we observed a chain of events that tied the P-cell's preferred direction of error in visual space to a vector of force production in motor space.

From these functional results we made an anatomical inference. The error preference in a region of sensory space, as signaled by the CSs, organized the P-cells into a computational unit that collectively predicted movement kinematics[4]. That preference for error also organized the downstream projections of the computational unit so that, through learning, the P-cells altered the motor output only along a vector that was parallel to their preferred error.

Results

We analyzed SSs and CSs of $n=67$ well-isolated P-cells from the oculomotor vermis of 7 monkeys in 187,008 trials. Each trial began with fixation on a visual target. After a random interval, the target was moved to a new location 10–25° away, resulting in a saccadic eye movement[16,24,25]. In most trials (~65%) the target was displaced during the saccade (Fig. 1a). In the remaining trials the target was not displaced, but inherent saccadic variability typically placed the eyes at a location other than the center of the target, resulting in a foveal error. In each trial we quantified the postsaccadic visual error as a vector that pointed from the eye location at saccade termination to the current target location.

Encoding of an error vector by complex spikes. When the saccade completed but the gaze did not land on the target, in the postsaccadic period P-cells produced a single CS with a probability that depended on the error direction (Fig. 1a and Supplementary Fig. 1). (The presence of two CSs in the 250-ms postsaccadic period was extremely rare, occurring in 0.33% of the CS present trials. In these cases we only considered the first CS.) For each P-cell, we labeled the error direction that produced the largest probability of CS as 'CS-on'[16]. Across the population, probability of CS was modulated

[1]Department of Biomedical Engineering, Laboratory for Computational Motor Control, Johns Hopkins University School of Medicine, Baltimore, MD, USA. [2]Department of Neurobiology, Duke University School of Medicine, Durham, NC, USA. [3]Department of Physiology and Biophysics, Washington National Primate Center, University of Washington, Seattle, WA, USA. *e-mail: david.herzfeld@duke.edu

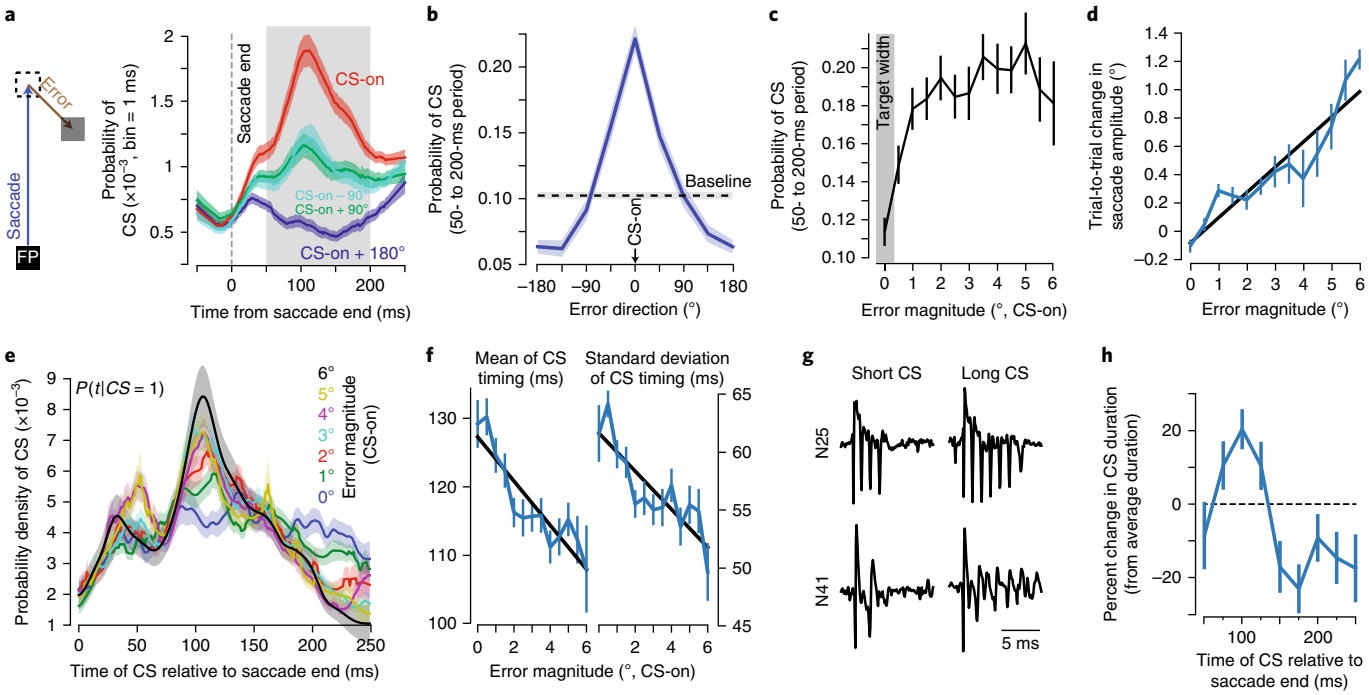

Fig. 1 | Error direction is encoded in the probability of CSs, whereas error magnitude modulates the distribution of CS timing. a, While the animal is gazing at a fixation point (FP), a target is presented (dashed square), and the animal makes a saccade toward it. During the saccade, in some trials, the target is displaced to another location (gray square), resulting in a visual error (the vector between eye position at saccade end and the target). Probability of CS across trials was computed for each millisecond of time for each P-cell and for various error directions. CS-on refers to direction of error vector that produced the highest probability of CS. **b**, Probability of CS in the 50- to 200-ms period (gray shading in **a**) following saccade end as a function of error direction. **c**, Probability of CS in the preferred error direction in the 50- to 200-ms period following saccade end as a function of error magnitude (error direction is CS-on). **d**, The amount of trial-to-trial behavioral learning as a function of error magnitude (best fit linear regression shown in black). **e**, Probability density of CS timing for a range of error magnitudes. Bin size is 1 ms. Error magnitude modulated the timing distribution, transforming it from uniform to unimodal. **f**, For each P-cell, we computed the probability density of CS timing (over the range 0–250 ms following saccade termination) for each error size, and then measured the mean and s.d. of each distribution. As error magnitude increased, both the mean and s.d. declined. Least squares fit to each measure is shown in black. **g**, CS waveforms for two representative P-cells. The duration of the CS waveform varied within each P-cell. **h**, Duration of the CS waveform as a function of when that CS was generated relative to saccade termination. Duration is expressed relative to each P-cell's mean CS duration. In all cases, error bars indicate between-cell variability via s.e.m. across all cells ($n = 67$).

by error direction (Fig. 1b). Errors in direction CS-on increased CS probability by 120.9 ± 10.1% with respect to baseline (the final 150 ms of the fixation period, before target motion, paired t test, $t_{66} = 12.17$; $P < 10^{-17}$), and errors in direction CS-on + 180° reduced this probability by 36.6 ± 5.2% (paired t test, $t_{66} = -7.32$; $P < 10^{-9}$). Therefore, the direction of the visual error was encoded in the probability of generating a CS, with each P-cell tuned to a preferred error direction.

In contrast, error magnitude did not modulate the probability of generating a CS (Fig. 1c), remaining invariant beyond 0.5° (repeated-measures (RM)-ANOVA, main effect of error magnitude $F_{10, 530} = 1.49$; $P = 0.14$). However, error magnitude clearly affected trial-to-trial change in behavior: on each trial we measured the component of the error vector along the direction of the primary target and then computed the trial-to-trial change in the amplitude of the saccade along that same direction. Larger errors produced larger trial-to-trial change in behavior (Fig. 1d; RM-ANOVA main effect of error magnitude $F_{6, 172} = 15.6$; $P < 0.001$). How could learning exhibit sensitivity to error magnitude when the signal that encoded that error in individual P-cells appeared to lack magnitude information?

We focused on trials in which an error occurred in direction CS-on and, for each P-cell, selected the subset of trials in which a CS occurred in the 250-ms postsaccadic period. We found that when the error was small, CS timing was distributed uniformly throughout the postsaccadic period (Fig. 1e). However, as error magnitude increased, CS timing transformed from a uniform to a unimodal distribution with a peak at ~110 ms. As a result, increased error magnitude coincided with a reduction in the s.d. (Fig. 1f; RM-ANOVA main effect of error magnitude, $F_{12, 489} = 5.74$; $P < 0.001$) and jitter of the CS timing distribution (Supplementary Fig. 2; median absolute distance from the median, RM-ANOVA, $F_{12, 515} = 4.39$; $P < 0.001$).

Notably, as CS timing changed, so did its waveform. In some instances, the duration of the CS waveform was short, whereas in other instances the same P-cell generated a longer-duration CS (Fig. 1g). We measured the duration of each CS and then computed how this duration varied within each P-cell as a function of CS timing (Fig. 1h). We found that CS timing predicted CS duration (Fig. 1h): a CS that occurred at 100 ms after saccade termination was about 20% longer in duration than average for that P-cell, whereas a CS that occurred at 200 ms after saccade termination was about 10% shorter in duration than average (Fig. 1h; one-sample t test comparing CS duration at 100 ms, $t_{66} = 3.7$; $P < 0.001$).

In summary, the direction of error modulated the probability of producing a CS in the postsaccadic period, whereas the magnitude of that error modulated the distribution of CS timing. As error magnitude increased, the temporal precision of CS production increased, focusing them in the 75- to 150-ms period. A CS that occurred during this window of time was different than CSs that occurred earlier or later: its waveform was longer in duration.

Behavioral change following occurrence of a complex spike. Even when the error was in direction CS-on, a P-cell produced a CS in only one-quarter of the trials (Fig. 1b). We sorted the data in a 2 × 2 design in which, after saccade completion, an error was either present or absent and the P-cell had either produced a CS or not. We measured change in behavior via the difference in motor output (time-series of eye velocity vectors) from the trial in which the error was experienced to the subsequent trial in which the same target was presented.

We began with trials in which the animal experienced an error in the CS-on direction of the P-cell (Fig. 2a). The probabilistic nature of CS produced a subset of trials in which the P-cell did not produce a CS in the postsaccadic period and another subset of trials in which the P-cell did produce a CS. As expected for both cases, in the subsequent trial the motor commands pulled the eyes more in the direction of error, coinciding with CS-on of the P-cell under study (Fig. 2a). The errors were similar in trials in which CS had or had not occurred (paired t test, $t_{66} = 1.25$; $P = 0.21$). However, the change in the motor output was larger, i.e., the pull was stronger, following production of a CS (Fig. 2a). A similar observation has been made in a different task (pursuit) when visual error was in direction CS-on of P-cells in the flocculus region of the cerebellum[21].

In some trials, the target was not moved during the saccade. As a result, the saccade terminated with the eyes on target, completing the movement without an error (|error| < 0.25°; Fig. 2b). Despite this lack of error, the probabilistic nature of CS produced trials in which the P-cell nevertheless generated a CS in the postsaccadic period. Notably, in the subsequent trial the gaze was again pulled in the CS-on direction of that P-cell (Fig. 2b). This biasing of behavior was missing when the P-cell did not produce a postsaccadic CS (Fig. 2b). Therefore, even without an error, the presence of a postsaccadic CS in a single P-cell was followed in the subsequent trial by a change in behavior: the gaze was pulled in the CS-on direction of that P-cell.

These results hinted that if a P-cell produced a postsaccadic CS, in the subsequent trial that P-cell (indirectly) influenced a specific group of motor neurons: those that produced force along the P-cell's CS-on direction. To test this hypothesis, we focused on trials in which error was in direction CS-on + 180° (i.e., error was opposite the preferred error direction of the P-cell). Following experience of this error, the behavior in the subsequent trial changed in the direction of that error (Fig. 2c). Notably, this learning was smaller if the P-cell had produced a CS. A similar pattern emerged when we considered trials in which error was in direction CS-on + 90° (Supplementary Fig. 3): trial-to-trial change in behavior was in direction of error, but the presence of a CS biased the motor commands in the CS-on direction. As a result, the difference between the trial-to-trial change in the motor commands that took place with and without a CS was always in direction CS-on, regardless of whether error was in direction CS-on (Fig. 2a), CS-on + 90° (Supplementary Fig. 3), CS-on + 180° (Fig. 2c), or absent altogether (Fig. 2b).

We therefore made our analysis blind to the error that the animal had actually experienced and instead labeled each trial based on whether the P-cell had or had not produced a postsaccadic CS. If the P-cell produced a CS, then the trial-to-trial change in saccade velocity vector was entirely in the CS-on direction of that P-cell (CS present; Fig. 2d), with no component along CS-on + 90°. In contrast, if the P-cell did not produce a CS, the trial-to-trial change was in direction CS-on + 180° of that P-cell (CS absent; Fig. 2d). Therefore, following production of a postsaccadic CS in a given P-cell, in the subsequent trial the gaze was pulled along a vector that was parallel to the CS-on direction of that P-cell. Without a CS, in the subsequent trial the gaze was pushed away along that same vector.

How did timing and/or shape of the CS affect these behaviors? If the CS was early (0–50 ms) or late (200–250 ms) with respect to saccade termination, in the subsequent trial there was little or no change in behavior (Fig. 2e). However, if the CS was produced in the 75- to 150-ms postsaccadic period, then the subsequent trial exhibited substantial changes (paired t test relative to no CS, $t_{66} = 4.9$; $P < 0.001$). Therefore, error magnitude affected CS timing (larger error made it more likely that a CS would occur 75–150 ms postsaccade; Fig. 1e), and CS timing affected trial-to-trial change in behavior.

However, CS timing also affected the duration of the CS waveform (Fig. 1h). We classified each CS as either 'long' or 'short' (a within-cell measure with respect to that cell's median CS waveform duration) and then quantified the effect of CS waveform duration as a function of CS timing. Once CS timing was accounted for, changes in CS duration produced no additional modulation of learning (Fig. 2f). This implied that the critical factor that modulated learning from error was CS timing.

Our trial-by-trial analysis imposed a specific coordinate system on the P-cells: their preferred direction of error, i.e., CS-on. What if we considered a different coordinate system, the preferred direction of SSs? For each P-cell we found the direction of saccade that produced the largest modulation in the SS response from baseline (see Methods) and then labeled all trials in which a CS had occurred during the postsaccadic period. We measured the trial-to-trial change in velocity and projected that change onto the SS preferred direction coordinate system. Using this coordinate system, we observed no meaningful change in behavior (Supplementary Fig. 4). Therefore, despite the fact that a P-cell influenced behavior via its SSs, it was the coordinate system with which that P-cell encoded error via its CS that revealed its role in influencing behavior.

These results allow us to conjecture about the anatomical organization of the P-cells in the oculomotor vermis and their downstream projections. About 50 P-cells project onto a single nucleus neuron[26], forming a microcluster. Functional[4] and anatomical[10,27–29] evidence suggests that P-cells of a microcluster share a common preference for error. When a saccade ends and a visual error is detected, there is increased probability of a postsaccadic CS in the microcluster that prefers that error direction. If the P-cells in that cluster produce a CS in the postsaccadic period, in the subsequent trial the motor output is biased via an increased pull in the CS-on direction of those P-cells. Following a trial without a postsaccadic CS, the bias is in the opposite direction. Therefore, it appears that a P-cell's SSs (indirectly) influence a population of motor neurons that produce a force parallel to that P-cell's direction of preferred visual error. That is, the direction of force in the motor space lies parallel to the direction of preferred error in the sensory space (Fig. 2g).

Simple spike change following experience of a complex spike. During a saccade, some P-cells exhibited a burst of SSs ('bursters'), while others exhibited a pause (Supplementary Fig. 5), with activity modulation that outlasted saccade duration (Fig. 3a). This diversity of activations is common for P-cells of the oculomotor vermis during saccadic movements[4,24,30,31] and for P-cells of the lateral cerebellum during wrist movements[32,33]. However, when we randomly sampled our cells into groups of 50 that shared the same preference for error and counted the SSs produced by the population, the population produced a response that predicted saccade velocity in real time[4] (Fig. 3a).

Following an error in direction CS-on, in the subsequent trial around saccade onset, there was a reduction in the SS discharge of both bursters and pausers (Fig. 3b). In contrast, following experience of an error in direction CS-on + 180°, there was an increase in the SS discharge of these cells. As a result, following experience of a CS-on error, the average change across all cells was a trial-to-trial decrease in the number of SSs (Fig. 3b), whereas following experience of a CS-on + 180° error, the average change was an increase.

Crucially, these changes in SSs were almost entirely dependent on whether the P-cell had produced a CS during the 50-ms window centered on the P-cell's median CS time (113.1 ± 14.6 ms,

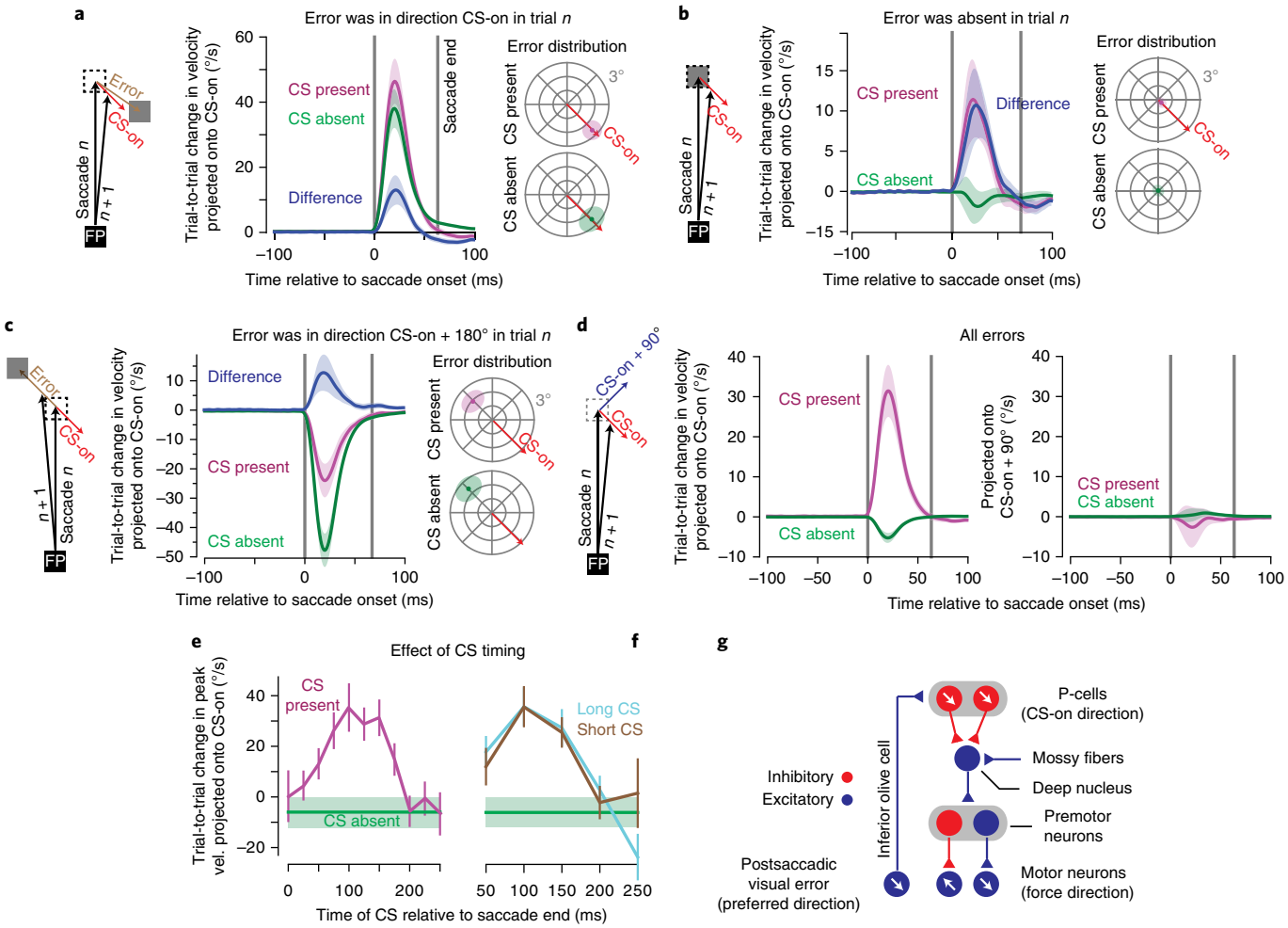

Fig. 2 | The influence of P-cell CSs on motor output. a, Analysis of trials in which the error was in the CS-on direction of the P-cell. We measured the eye trajectory (velocity vectors as a function of time) during the saccade in the trial in which the error was experienced, as well as the trajectory in the subsequent trial in which a saccade was made to the same target. To measure change in behavior, we projected the difference in the two-dimensional sequence of velocity vectors onto the CS-on direction of the P-cell. Following experience of an error, the next trial exhibited an increase in the velocity vector along the direction of error. However, if the P-cell produced a CS, velocity on the next trial was larger in direction CS-on compared to when a CS was absent (mean + s.e.m. across neurons). Distribution of errors for CS present and CS absent trials were comparable (right, shaded region denotes average s.d. of error distribution across neurons). **b**, As in **a**, except for trials in which there was no postsaccadic error (|error| < 0.25°). Even without an error, presence of a CS led to increased motor output along direction CS-on of the P-cell that had produced the CS. **c**, As in **a**, except for trials in which errors were in CS-on + 180° of the P-cell under study. Even when the error was opposite the preferred direction, presence of a CS biased behavior in CS-on direction of that cell. **d**, Trial-to-trial change following any error. We projected the trial-to-trial change in velocity onto direction CS-on (left) and CS-on + 90° (right) of the P-cell. When a CS was present, change in motor output was only in direction CS-on. **e**, A CS during a specific postsaccadic period (~75–150 ms) resulted in more learning than earlier or later CSs. **f**, Effect of CS waveform duration. For each P-cell, we classified each CS as long or short with respect to median duration within each cell. At a given CS timing, CS waveform duration did not have a discernible effect on behavior. **g**, Hypothesized anatomy of the oculomotor vermis P-cells and cerebellar output. Red circles, inhibitory neurons; blue circles, excitatory neurons. Arrows indicate preferred error vector in sensory space for the inferior olive and P-cells and indicate direction of force for the motor neurons. The vectors are parallel in the sensory and motor spaces. All error bars are s.e.m. across all neurons ($n = 67$) unless noted.

mean ± s.d.). For bursters and pausers, as well as all cells together, a CS in this temporal window was followed in the subsequent trial by a reduction in the SSs (Fig. 3c). However, despite experience of error, if no CS occurred in this temporal window, in the subsequent trial there was little or no change in the SSs. These results are consistent with observations made in the flocculus during visual pursuit[7,8] and vestibulo-ocular adaptation[9], demonstrating that in different regions of the cerebellum, presence of a CS leads to trial-to-trial suppression in the number of SSs produced by the P-cells.

We next quantified the trial-to-trial change in SSs (Fig. 3d) and behavior (Fig. 3e) as a function of timing of the postsaccadic CS. For each P-cell, we computed the median of its CS timing distribution in the postsaccadic period (113.1 ± 14.6 ms, mean of the median ± s.d.) and then measured the trial-to-trial change in the SSs with respect to this median. If the CS occurred early (<25 ms before the median CS time for that P-cell) or late (>25 ms after the median), in the following trial there was little or no change in the SSs of the population. However, if the CS occurred in the median period (median ± 25 ms), there was a reduction in the SSs. Furthermore, this median period was critical for inducing a change in behavior: trial-to-trial changes in saccade velocity were largest following a CS that occurred at the median postsaccadic period (Fig. 3d). Absence of a CS also influenced the SSs. After consecutive no-CS trials, there was an increase in the SSs (Fig. 3d).

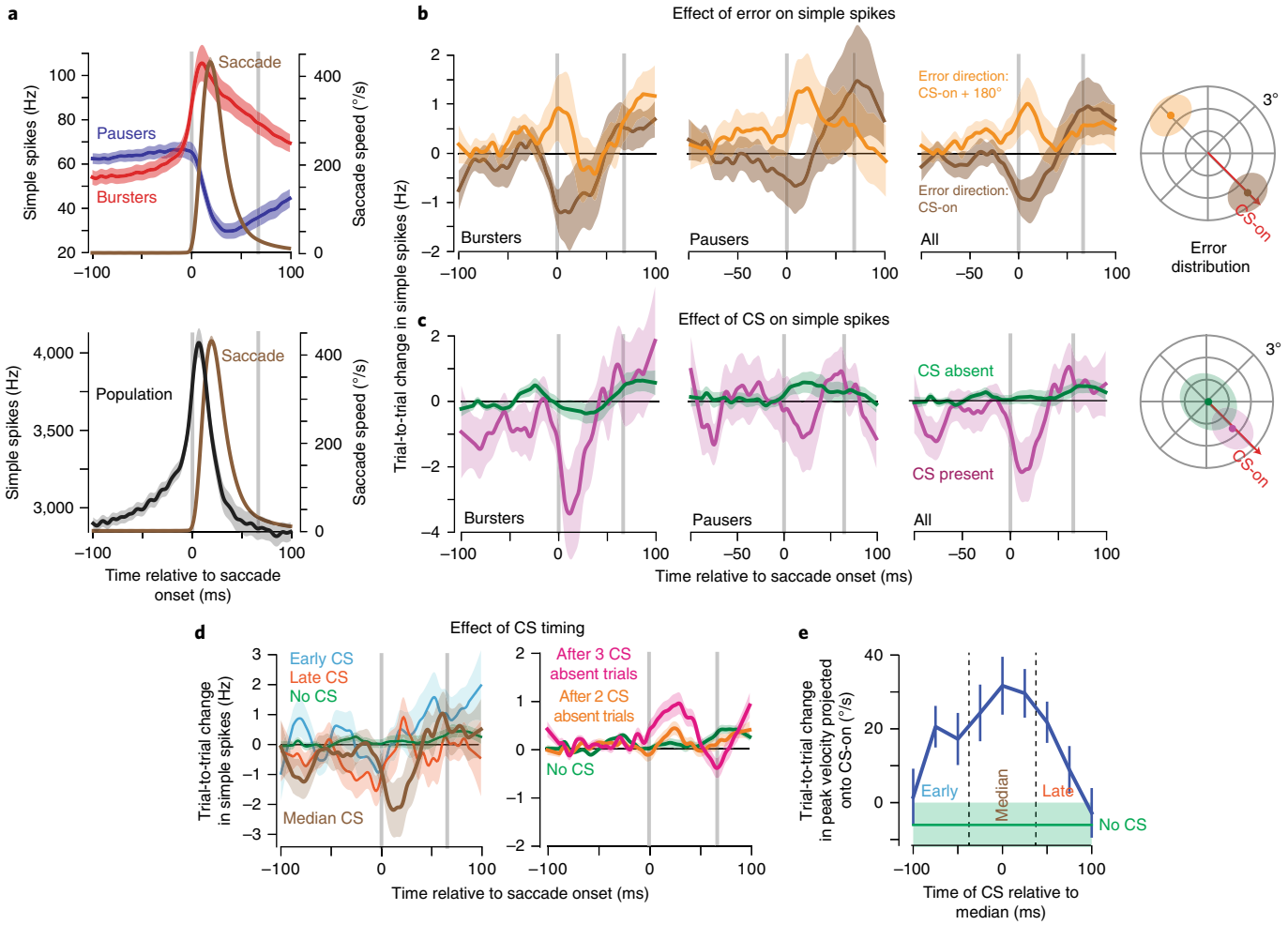

Fig. 3 | CSs cause trial-to-trial depression in SS responses. a, Top: average activity for all bursting (red) and pausing (blue) cells. Vertical gray lines indicate saccade onset and termination. Bottom: while neither of the subpopulations in the top graph predict eye speed in real time, their combined activity in a population predicts the real-time speed of the eye[4]. **b**, Effect of error on SSs. Following an error in CS-on (high probability of CS), both burst and pause cells reduced their activity, whereas when the probability of CS was low (CS-on + 180°), these cells increased their activity. The mean response across P-cells showed trial-to-trial changes that paralleled the responses of burst and pause cells. **c**, Effect of CS on SSs. When a CS was present within 25 ms of the median CS response time in the postsaccadic period, SSs changed in the next trial for bursters, pausers, and across all cells (magenta), whereas when a CS was absent (green), there was little or no change in SS response on the next trial. **d**, CS timing played a critical role in changing the SSs. If the CS occurred during a temporal window of 50 ms centered on the median CS time, it produced larger trial-to-trial change in SSs (brown) than if the CS occurred earlier (cyan) or later (red) than this time period. Lack of a CS (green) in a single trial was followed by little or no change in the SSs. Persistent lack of a CS in two (green) or three (red) trials resulted in increased SSs. **e**, A CS that occurred around the median period was most effective in producing trial-to-trial change in behavior. In all cases, median timing refers to a within-cell measure of postsaccadic distribution of CS timing. All error bars are s.e.m. across $n = 67$ P-cells, except in **a** where it reflects 95% confidence interval about the mean of bootstrap population of 50 randomly selected P-cells. SS data were smoothed with a Savitzky–Golay filter with a width of 25 ms.

In summary, during a saccade some P-cells modulated their SS response via a burst, while others modulated their response via a pause. In both groups, as well as the population, the experience of a CS was followed on the subsequent trial by a reduction in the rate of SSs. In contrast, lack of a CS was followed by an increase in the SSs. The effect of a CS on the SSs, as well as on behavior, depended on timing: a CS that was generated in the postsaccadic period had its largest influence when it occurred at the median of the timing distribution, at around 110 ms.

Bidirectional change in P-cell simple spikes during learning. In theory, with repetition, the trial-by-trial changes in the SSs should accumulate to produce large-scale changes in behavior. However, previous studies have provided conflicting evidence of SS changes during blocks of adaptation. While one study reported that the changes in peak discharge appeared unrelated to changes in behavior during bouts of adaptation[34], a second study suggested that there are coherent SS changes[24]. To shed light on this puzzle, we trained the monkeys in a 'gain-down' protocol: on every trial, following saccade onset, the target was moved inward. By necessity, in some trials the primary saccade was in direction CS-on of the P-cell under study, while in other trials the primary saccade was in direction CS-on + 180° of the same cell (total of 1,069 ± 89 trials per neuron, mean ± s.e.m.). This training produced consistent reductions in saccade velocity and amplitude for both directions of movement (Fig. 4a; velocity: RM-ANOVA, main effect of adaptation trials $F_{9,\,1,098} = 13.5$; $P < 0.001$).

The two directions of primary saccade implied that in some trials the postsaccadic error was in CS-on direction of the P-cell, whereas in other trials the error was in CS-on + 180° (Fig. 4a). We therefore organized the P-cells into populations of 50 based on their preferred

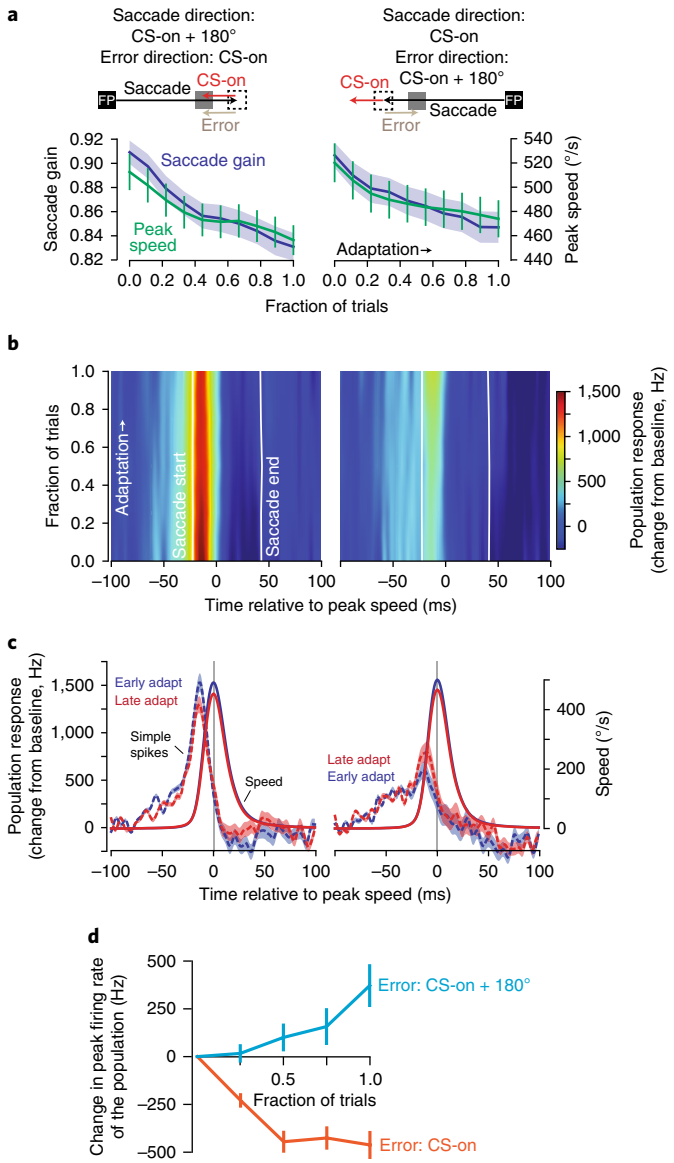

Fig. 4 | Persistent errors in a saccadic gain-down experiment produce bidirectional changes in SSs. a, Adaptation protocol. Saccades occurred in two directions. For both directions, the target was moved inward on saccade initiation. As a result, in some trials the postsaccadic error was in direction CS-on (left), while in other trials the error was in CS-on + 180° (right). Regardless of saccade or error direction, saccade gain (saccade amplitude divided by target amplitude) and saccade peak velocity declined with training. On average, the number of trials for each direction was 535 ± 45 (mean ± s.e.m.). Error bars show s.e.m. across adaptation sessions for all cells ($n = 67$). **b**, We organized the cells based on their CS-on direction. The plots show change in population response during adaptation, with respect to baseline. Data in the amplitude axis were smoothed by a first-order Savitzky–Golay filter with a width of 3 bins. **c**, When errors were in direction CS-on, the population response decreased during adaptation. When errors were in direction CS-on + 180°, the population response in the same cells increased. Error bars show 95% confidence intervals about the mean for bootstrap population of 50 cells. **d**, Change in peak response of the population relative to baseline from beginning to end of adaptation. Error bars show 95% confidence about the mean interval for bootstrap population of 50 cells.

error direction. In early trials, the SS response of the population was strong when the primary saccade was in direction CS-on + 180° and weak when that saccade was in direction CS-on (Fig. 4c). This is consistent with the idea that the SSs of the population encode motion of the eyes during a saccade via a gain-field[4], wherein the gain of SSs generated by the population is largest for saccades in direction CS-on + 180°.

Despite the fact that velocity and amplitude decreased for both directions of the primary saccades, the population response changed in a way that depended on whether the postsaccadic errors were in direction CS-on or CS-on + 180°. When the saccade was in direction CS-on + 180°, the postsaccadic error vector was in direction CS-on (increased probability of CS). For this movement direction, the SS response of the population declined with adaptation (Fig. 4b,c). However, when the saccade was in direction CS-on, the postsaccadic error vector was in direction CS-on + 180° (decreased probability of CS). For this movement direction, the SS response of the same P-cells increased (Fig. 4b,c). That is, change in the SS response was modulated by the direction of the experienced error (RM-ANOVA with main effect of error direction $F_{1,98} = 111.9$, $P < 10^{-15}$; main effect of trial $F_{4,392} = 21.0$, $P < 10^{-15}$; and direction-by-trial interaction $F_{4,392} = 134.3$, $P < 10^{-15}$). Therefore, when P-cells were organized based on their preference for error, the population SS response encoded the motion of the eyes during a saccade via a gain-field[4]. With training, the gain of this encoding simultaneously changed in two different directions: increasing for saccades in direction CS-on (because the postsaccadic error was in direction CS-on + 180°) and decreasing for saccades in direction CS-on + 180 (because the postsaccadic error was in direction CS-on; Fig. 4d).

The simultaneous, bidirectional changes we observed in P-cells during a single training session provide a rationale for why, in a previous saccade gain-down adaptation study, little or no change was observed in SS rates[34]: if we did not organize the P-cells based on their preference for error, the changes in the population responses for the two opposing directions canceled, producing no obvious changes in SS rates despite changes in behavior (Supplementary Fig. 6). However, when the directionality of the error preference is taken into account[24], clear changes in the SS response can be uncovered.

Discussion

There is disparity between the simple spikes' rich representation of predictions about the ongoing movement and the complex spikes' sparse representation of error in those predictions. How can P-cells learn control of behavior from the infrequent occurrence of a CS?

We found that in the oculomotor vermis, after a saccadic eye movement, the direction of the visual error vector affected the probability of the postsaccadic CS (with each P-cell having a preference for an error direction[16]). In contrast, error magnitude affected CS timing, making it less variable, clustering the CSs around 110 ms after saccade termination as the error magnitude grew larger. The CSs that occurred around this time had waveforms that were longer in duration. They induced greater plasticity in the SSs, and they produced greater trial-to-trial change in behavior. The chain of events that began with production of a CS in a single P-cell culminated in a specific change in behavior on the subsequent trial: the movement was biased along a force vector that was parallel to the preferred visual error vector of the parent P-cell.

If during the postsaccadic period the P-cell did not produce a CS, in the subsequent trial the gaze was pushed away along a vector that was also parallel to the CS-on direction of that cell. These results explain why, during the progression of gain-down adaptation, wherein the saccade velocity and amplitude decreased for all directions of movement, for some directions the SS response increased while for other directions the response of the same P-cells decreased: the bidirectional changes in SSs were driven by postsaccadic errors that changed direction with respect to the P-cell's preferred error.

In current models employed for decoding neuronal activity in the motor system, cells are placed into populations based on their

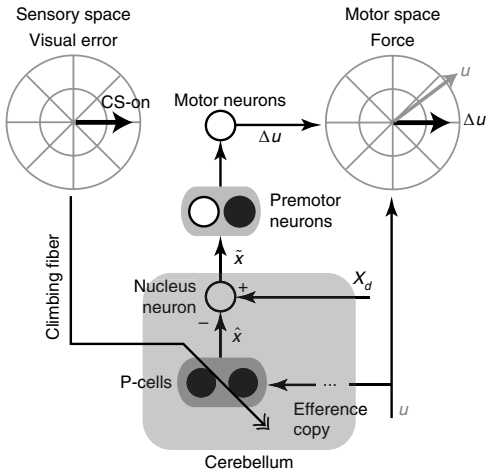

Fig. 5 | Transformation of a sensory error into a subsequent change in behavior in the oculomotor vermis. Experience of a visual error in the postsaccadic period increases the probability of generating a CS in a population of P-cells that prefer that error direction. If a CS is generated, it causes plasticity in the P-cells, modifying the SSs that are produced collectively by the population, altering their prediction of state $\hat{x}$. At the deep cerebellar nucleus cell, the predicted state is an inhibitory signal that is compared with an excitatory signal from the mossy fibers, which possibly carry information about the desired state x_d. The output of the nucleus neuron is the difference between these two variables, reflecting a state correction x associated with the ongoing motor command u. This correction affects motor behavior in a specific direction: the direction of force specified by vector Δu. The preferred direction of visual error that produced a CS in the P-cells (i.e., CS-on) is parallel to the direction of force Δu in the effectors that the P-cells project to. Black circles, inhibitory neurons; white circles, excitatory neurons.

patterns of spikes, for example, via tuning with respect to direction of movement[35] or covariance of their activity with respect to a behavioral variable[36]. In contrast, our results suggest that in the cerebellum, P-cells form populations that may be difficult to infer based on their patterns of activity (SSs), but easy to organize based on their preference for error.

In the oculomotor vermis, P-cells may be organized into populations that share the same preference for error[4,10,27–29]. Here our results suggest that this preference for error also organizes the projections of each population onto the motor space: the vector of preferred error in visual space predicts the influence of those P-cells in movement space (Fig. 5). To explain this idea, consider that in the oculomotor vermis, P-cells project onto cells in the caudal fastigial nucleus (cFN). cFN cells project to interneurons in the brainstem (burst generators)[37,38], which in turn project to motor neurons. Our results imply that a cFN neuron does not project to random premotor neurons, but only those that activate motor neurons that pull the gaze in the CS-on direction of the parent P-cells.

The resulting circuit (Fig. 5) functions as an adaptive controller: experience of an error is encoded as a sensory event that affects CS probability and timing. The purpose of the controller is to nullify the error, returning the CS probability back to baseline. It accomplishes this by relying on the wiring of the P-cells: their discharge (indirectly) influences activity of effectors whose direction of action in motor space is parallel to the direction of preferred error in sensory space.

When an error occurs, for some P-cells this error will be in direction CS-on, while for others this error will be in direction CS-on + 180°. Therefore, on the subsequent trial some clusters of P-cells will increase their SSs, while others will decrease their response. At the level of cerebellar output, do these changes counteract or cooperate with each other?

Our anatomical inference in Fig. 2g, coupled with functional changes reported in Figs. 3 and 4 and the known anatomy of cerebellar[39] and inferior olive projections[40], present a solution. When a saccade takes place and the error is to the left (Supplementary Fig. 7), following saccade completion, the leftward visual error vector engages the right superior colliculus, which in turn engages the left inferior olive. This upregulates CS production in P-cells on the right side of the vermis and downregulates CS production in P-cells on the left side of the vermis. On the subsequent trial, P-cells with leftward CS-on will decrease their SS response, indirectly increasing the discharge in the motor neurons that pull to the left[41]. However, P-cells that have a rightward CS-on preference will increase their SS response, resulting in a reduced drive to the motor neurons that pull to the right. That is, despite their opposite preferences for error, and opposite changes in their SSs, the two clusters of P-cells will cooperate to alter the drive to the agonist and antagonist motor neurons, reducing the error.

A cerebellar microcircuit is thought to be a group of P-cells that receive climbing fiber inputs that share the same preference for sensory input and innervate a specific subset of cells in the deep nucleus that may have a similar output function[42,43]. Our results provide functional evidence that P-cells likely organize into computational units that not only share the same preference for error, but also influence behavior through their projections, by acting on effectors that specifically reduce that error. While individual P-cells produce disparate patterns of SSs during a given movement[24,30,44], those that prefer the same error may collectively form a single computational unit, influencing effectors that can contribute to homeostatic regulation of the unit's complex spikes[45].

Methods

Methods, including statements of data availability and any associated accession codes and references, are available at https://doi.org/10.1038/s41593-018-0136-y.

Received: 3 October 2017; Accepted: 7 March 2018;
Published online: 16 April 2018

References

1. Shidara, M., Kawano, K., Gomi, H. & Kawato, M. Inverse-dynamics model eye movement control by Purkinje cells in the cerebellum. *Nature* **365**, 50–52 (1993).
2. Krauzlis, R. J. & Lisberger, S. G. SS responses of gaze velocity Purkinje cells in the floccular lobe of the monkey during the onset and offset of pursuit eye movements. *J. Neurophysiol.* **72**, 2045–2050 (1994).
3. Dash, S., Catz, N., Dicke, P. W. & Thier, P. Encoding of smooth-pursuit eye movement initiation by a population of vermal Purkinje cells. *Cereb. Cortex* **22**, 877–891 (2012).
4. Herzfeld, D. J., Kojima, Y., Soetedjo, R. & Shadmehr, R. Encoding of action by the Purkinje cells of the cerebellum. *Nature* **526**, 439–442 (2015).
5. Roitman, A. V., Pasalar, S., Johnson, M. T. V. & Ebner, T. J. Position, direction of movement, and speed tuning of cerebellar Purkinje cells during circular manual tracking in monkey. *J. Neurosci.* **25**, 9244–9257 (2005).
6. Hewitt, A. L., Popa, L. S., Pasalar, S., Hendrix, C. M. & Ebner, T. J. Representation of limb kinematics in Purkinje cell simple spike discharge is conserved across multiple tasks. *J. Neurophysiol.* **106**, 2232–2247 (2011).
7. Medina, J. F. & Lisberger, S. G. Links from complex spikes to local plasticity and motor learning in the cerebellum of awake-behaving monkeys. *Nat. Neurosci.* **11**, 1185–1192 (2008).
8. Yang, Y. & Lisberger, S. G. Role of plasticity at different sites across the time course of cerebellar motor learning. *J. Neurosci.* **34**, 7077–7090 (2014).
9. Kimpo, R. R., Rinaldi, J. M., Kim, C. K., Payne, H. L. & Raymond, J. L. Gating of neural error signals during motor learning. *eLife* **3**, e02076 (2014).
10. Fujita, H. & Sugihara, I. Branching patterns of olivocerebellar axons in relation to the compartmental organization of the cerebellum. *Front. Neural Circuits* **7**, 3 (2013).
11. Marr, D. A theory of cerebellar cortex. *J. Physiol. (Lond.)* **202**, 437–470 (1969).
12. Albus, J. S., Branch, D. T., Donald, C. & Perkel, H. A theory of cerebellar function. *Math. Biosci.* **10**, 25–61 (1971).

13. Kitazawa, S., Kimura, T. & Yin, P.-B. Cerebellar complex spikes encode both destinations and errors in arm movements. *Nature* **392**, 494–497 (1998).
14. Keating, J. G. & Thach, W. T. Nonclock behavior of inferior olive neurons: interspike interval of Purkinje cell complex spike discharge in the awake behaving monkey is random. *J. Neurophysiol.* **73**, 1329–1340 (1995).
15. Ke, M. C., Guo, C. C. & Raymond, J. L. Elimination of climbing fiber instructive signals during motor learning. *Nat. Neurosci.* **12**, 1171–1179 (2009).
16. Soetedjo, R., Kojima, Y. & Fuchs, A. F. Complex spike activity in the oculomotor vermis of the cerebellum: a vectorial error signal for saccade motor learning? *J. Neurophysiol.* **100**, 1949–1966 (2008).
17. Ojakangas, C. L. & Ebner, T. J. Purkinje cell complex and simple spike changes during a voluntary arm movement learning task in the monkey. *J. Neurophysiol.* **68**, 2222–2236 (1992).
18. Maruta, J., Hensbroek, R. A. & Simpson, J. I. Intraburst and interburst signaling by climbing fibers. *J. Neurosci.* **27**, 11263–11270 (2007).
19. Mathy, A. et al. Encoding of oscillations by axonal bursts in inferior olive neurons. *Neuron* **62**, 388–399 (2009).
20. Najafi, F., Giovannucci, A., Wang, S. S.-H. & Medina, J. F. Coding of stimulus strength via analog calcium signals in Purkinje cell dendrites of awake mice. *eLife* **3**, e03663 (2014).
21. Yang, Y. & Lisberger, S. G. Purkinje-cell plasticity and cerebellar motor learning are graded by complex-spike duration. *Nature* **510**, 529–532 (2014).
22. Yang, Y. & Lisberger, S.G. Modulation of complex-spike duration and probability during cerebellar motor learning in visually guided smooth-pursuit eye movements of monkeys. *eNeuro* https://doi.org/10.1523/ENEURO.0115–17.2017 (2017).
23. Suvrathan, A., Payne, H. L. & Raymond, J. L. Timing rules for synaptic plasticity matched to behavioral function. *Neuron* **92**, 959–967 (2016).
24. Kojima, Y., Soetedjo, R. & Fuchs, A. F. Changes in simple spike activity of some Purkinje cells in the oculomotor vermis during saccade adaptation are appropriate to participate in motor learning. *J. Neurosci.* **30**, 3715–3727 (2010).
25. Soetedjo, R. & Fuchs, A. F. Complex spike activity of purkinje cells in the oculomotor vermis during behavioral adaptation of monkey saccades. *J. Neurosci.* **26**, 7741–7755 (2006).
26. Person, A. L. & Raman, I. M. Purkinje neuron synchrony elicits time-locked spiking in the cerebellar nuclei. *Nature* **481**, 502–505 (2011).
27. De Zeeuw, C. I. et al. Spatiotemporal firing patterns in the cerebellum. *Nat. Rev. Neurosci.* **12**, 327–344 (2011).
28. Heck, D. H., De Zeeuw, C. I., Jaeger, D., Khodakhah, K. & Person, A. L. The neuronal code(s) of the cerebellum. *J. Neurosci.* **33**, 17603–17609 (2013).
29. Tang, T., Suh, C. Y., Blenkinsop, T. A. & Lang, E. J. Synchrony is key: complex spike inhibition of the deep cerebellar nuclei. *Cerebellum* **15**, 10–13 (2016).
30. Helmchen, C. & Büttner, U. Saccade-related Purkinje cell activity in the oculomotor vermis during spontaneous eye movements in light and darkness. *Exp. Brain Res.* **103**, 198–208 (1995).
31. Raghavan, R. T. & Lisberger, S. G. Responses of Purkinje cells in the oculomotor vermis of monkeys during smooth pursuit eye movements and saccades: comparison with floccular complex. *J. Neurophysiol.* **118**, 986–1001 (2017).
32. Ishikawa, T. et al. Releasing dentate nucleus cells from Purkinje cell inhibition generates output from the cerebrocerebellum. *PLoS One* **9**, e108774 (2014).
33. Mano, N. & Yamamoto, K. Simple-spike activity of cerebellar Purkinje cells related to visually guided wrist tracking movement in the monkey. *J. Neurophysiol.* **43**, 713–728 (1980).
34. Catz, N., Dicke, P. W. & Thier, P. Cerebellar-dependent motor learning is based on pruning a Purkinje cell population response. *Proc. Natl. Acad. Sci. USA* **105**, 7309–7314 (2008).
35. Georgopoulos, A. P., Schwartz, A. B. & Kettner, R. E. Neuronal population coding of movement direction. *Science* **233**, 1416–1419 (1986).
36. Stavisky, S. D., Kao, J. C., Ryu, S. I. & Shenoy, K. V. Trial-by-trial motor cortical correlates of a rapidly adapting visuomotor internal model. *J. Neurosci.* **37**, 1721–1732 (2017).
37. Scudder, C. A., Fuchs, A. F. & Langer, T. P. Characteristics and functional identification of saccadic inhibitory burst neurons in the alert monkey. *J. Neurophysiol.* **59**, 1430–1454 (1988).
38. Strassman, A., Highstein, S. M. & McCrea, R. A. Anatomy and physiology of saccadic burst neurons in the alert squirrel monkey. II. Inhibitory burst neurons. *J. Comp. Neurol.* **249**, 358–380 (1986).
39. Noda, H., Sugita, S. & Ikeda, Y. Afferent and efferent connections of the oculomotor region of the fastigial nucleus in the macaque monkey. *J. Comp. Neurol.* **302**, 330–348 (1990).
40. Sugihara, I., Wu, H. & Shinoda, Y. Morphology of single olivocerebellar axons labeled with biotinylated dextran amine in the rat. *J. Comp. Neurol.* **414**, 131–148 (1999).
41. Kojima, Y., Robinson, F. R. & Soetedjo, R. Cerebellar fastigial nucleus influence on ipsilateral abducens activity during saccades. *J. Neurophysiol.* **111**, 1553–1563 (2014).
42. Dean, P. & Porrill, J. The cerebellum as an adaptive filter: a general model? *Funct. Neurol.* **25**, 173–180 (2010).
43. Bengtsson, F. & Jörntell, H. Specific relationship between excitatory inputs and climbing fiber receptive fields in deep cerebellar nuclear neurons. *PLoS One* **9**, e84616 (2014).
44. Thier, P., Dicke, P. W., Haas, R. & Barash, S. Encoding of movement time by populations of cerebellar Purkinje cells. *Nature* **405**, 72–76 (2000).
45. Mauk, M. D. & Donegan, N. H. A model of Pavlovian eyelid conditioning based on the synaptic organization of the cerebellum. *Learn. Mem.* **4**, 130–158 (1997).

Acknowledgements

These data were collected in the laboratory of A. Fuchs. The authors are very grateful for his generosity. The work was supported by NIH grants R01NS078311 (R. Shadmehr), R01EY019258 (R. Soetedjo), R01EY023277 (Y.K.), the Johns Hopkins Science of Learning Institute (D.J.H.), and the Office of Naval Research (N00014-15-1-2312, R. Shadmehr).

Author contributions

Y.K. and R. Soetedjo conceived, designed, and performed all experiments. D.J.H. analyzed the data and made all figures. R. Shadmehr and D.J.H. wrote the paper.

Competing interests

The authors declare no competing interests.

Additional information

Supplementary information is available for this paper at https://doi.org/10.1038/s41593-018-0136-y.

Reprints and permissions information is available at www.nature.com/reprints.

Correspondence and requests for materials should be addressed to D.J.H.

Publisher's note: Springer Nature remains neutral with regard to jurisdictional claims in published maps and institutional affiliations.

Methods

Animals. We analyzed saccade data from $n=67$ well-isolated P-cells from the oculomotor vermis of the cerebellum in 7 rhesus monkeys (*Macaca mulatta*, all males 5.0–7.4 kg: B, F, W, K, KO, P, and O). No statistical methods were used to predetermine sample sizes. Animals were not randomized into separate groups. All experiments were performed in accordance with the *Guide for the Care and Use of Laboratory Animals* (1997) and exceeded the minimal requirements recommended by the Institute of Laboratory Animal Resources and the Association for Assessment and Accreditation of Laboratory Animal Care International. All animal procedures were approved by the local Animal Care and Use Committee at the University of Washington.

General procedures. The experimental dataset and methodology have been published previously[16,24,25]. Briefly, the right eyes of 7 rhesus monkeys were surgically implanted with a scleral search coil and a restraint lug under aseptic conditions. Following recovery from the procedure, the monkeys were placed in a magnetic field, allowing measurement of eye kinematics (position and velocity) at 1 kHz while the head was held stationary[46]. Monkeys were trained to make visually guided saccades to a target dot (<0.4° in diameter) in a dimly lit room. The target spot moved to a new location at a rate of approximately 1 Hz. Targets were either presented via light emitting diodes (LEDs), which were placed at 1° eccentricities from center in eight directions (45° spacing) or via a red laser beam whose position was controlled by two mirror galvanometers. All targets appeared within ±30° of straight ahead. Monkeys were continuously rewarded with applesauce for keeping their gaze within a virtual bounding box that extended ±3° in both the horizontal and vertical directions.

Once the monkey demonstrated proficiency tracking targets of various amplitudes and directions for an extended period of time (>2 h), each monkey underwent a second aseptic surgical procedure to implant a recording chamber, which provided access to the oculomotor vermis (lobules VI and VII) of the cerebellum. The chamber was located on the midline, 14.5 mm posterior to the intraoral axis, and directed straight down. Following recovery from surgery, we inserted single custom tungsten microelectrodes into OMV. The electrodes were coated with iron particles to reduce their impedance to approximately 100 kΩ at 1 kHz. We recognized penetration of OMV by the characteristic saccade-related 'swooshing' in background activity. We identified single P-cells using three criteria: (i) the presence of high frequency saccade-related SS activity, (ii) the presence of multipeaked CSs, and (iii) the presence of a CS-linked pause in the SSs. We simultaneously recorded neurophysiology (50 kHz sampling rate) and eye kinematics (1 kHz sampling rate) via a Cambridge Electronic Design Power 1401. Data was displayed in real time to the experimenter on a computer monitor running Spike2, as well as saved for offline analysis.

Complex spike identification and processing. Neurophysiology data were bandpass-filtered between 30 Hz and 10 kHz before analysis. We used a semiautomated procedure to identify complex spikes from the recorded data. Briefly, the experimenter, blind to the animal's behavior, manually identified a subset of complex spikes for each recording. We then used a template-matching algorithm to identify onset of the complex spike waveform throughout the experimental session. Our template-matching algorithm was intentionally strict, attempting to minimize the number of false-positive identifications (i.e., SSs categorized as complex spikes). However, this procedure has the necessary consequence of potentially missing a small fraction of complex spikes (false negatives). Blind to the animal's behavior, we intentionally excluded P-cells that did not consistently produce complex spikes throughout the entire recording period, indicating that the P-cell recording was not stable.

After the algorithm identified the onset of each complex spike, we also sought to identify the duration of that spike. For each complex spike identified in the 50- to 250-ms period following saccade termination, a single experimenter (D.J.H.) determined the duration of the complex spike waveform by manually marking termination of each waveform. The experimenter was blind to the animal's behavior and the time of the complex spike within this 200-ms postsaccadic period. The times of all identified complex spikes were downsampled to 1 kHz, corresponding to the sampling rate of the behavioral data.

After complex spike identification, we performed sorting on the Purkinje cell SSs and subsequently downsampled the SS times to 1 kHz. To convert SSs to instantaneous firing rates, we noncausally convolved each spike train with a normalized Gaussian kernel with a 2.5-ms s.d. (area of the kernel was normalized to 1.0). We included $n=67$ P-cells in our final dataset that had well-isolated examples of both simple and complex spike responses for the duration of the recording session. No P-cells were excluded based on the animal's behavior.

Behavioral data processing. We identified potential saccadic events via an absolute speed threshold of 100°/s. The onset of these potential saccades was determined by finding the time at which the eye speed exceeded 20°/s for more than 3 ms. Similarly, the end of the saccade was defined as the time when eye speed fell below 20°/s for more than 3 ms. For each saccade, we identified the maximum absolute speed during the saccadic period. Trials in which the monkey moved its eyes in the wrong direction relative to the target (>90°) or trials in which the endpoint of the saccade landed more than 10° from the target location were excluded from further analysis (less than 5% of all trials).

In some cases, we induced a 3–5° postsaccadic visual error by displacing the target during the saccade. However, even when we did not move the target, the natural variability of eye movements resulted in postsaccadic errors. For each saccade, regardless of whether the target was displaced or not, we determined a postsaccadic foveal error vector from the monkey's eye position at saccade termination to the center of the current target position. When the target was not displaced during the saccade, the average error magnitude was 2.0 + 0.1° (mean + s.e.m.), indicating that the monkey made errors even without intrasaccadic perturbation of the target.

Determination of CS and SS preferred directions. After identification of postsaccadic errors and complex spike timing for each P-cell, we determined the preferred direction of complex spikes (CS-on) for each P-cell. For each trial, we labeled the presence or absence of a complex spike in a 50- to 200-ms window following saccade termination[4,16]. However, if a corrective saccade occurred during the 50- to 200-ms window, we used the onset of the corrective saccade as the end of the CS window.

To determine CS-on, we divided postsaccadic errors across the experiment into eight directions, spaced at 45° intervals. For each direction of error, we determined the probability of a CS during the postsaccadic period (number of trials with a given error direction and a CS, divided by the total number of trials with that error direction). The error direction with the highest probability of CS was labeled 'CS-on'. An example of this CS tuning profile for an individual neuron is shown in Supplementary Fig. 1. We have previously shown that the probability of CS during the postsaccadic period depends on the direction of the postsaccadic error and not the direction of the preceding saccade[4].

For each cell we also determined the SS preferred direction. Here, we divided trials into eight directions based on the direction of the animal's saccade toward the presented target. For each trial, we determined the average instantaneous firing rate during the saccadic period (from saccade onset to saccade offset). In addition, we determined the average SS firing rate during a baseline period 200- to 50-ms before saccade onset. We labeled the preferred SS direction (SS-on) as the saccade direction that elicited the largest absolute firing rate change from baseline, i.e., the direction with the largest modulation from baseline activity. In other regions of the cerebellum (for example, the flocculus), there is an inverse relationship between the preferred direction of SSs and the preferred direction of CS[47]. However, similarly to previous studies in OMV, we found no evidence for such a link between these two preferred directions[31]. Rather, the distribution of angular difference between SS and CS preferred directions were not significantly different than an expected uniform distribution ($\chi^2(7, n=67)=2.37$; $P=0.94$).

Lack of encoding of error magnitude in probability of CS. In Fig. 1c, we asked whether foveal error magnitude was encoded in the probability of CS during the 50- to 200-ms following saccade termination. We quantified the encoding of error magnitude along a single axis: each P-cell's CS-on direction. Here positive errors occurred in CS-on and negative errors occurred in the opposite direction, CS-on + 180°. By necessity, the probability of complex spikes must pass through the P-cell's baseline probability of CS when the error magnitude is 0°. To address whether there was a significant encoding of error magnitude in CS probability, we binned error magnitudes along the CS-on axis from 0° to 6° into 0.5° discrete bins. For each bin, we computed the probability of a CS occurring in the postsaccadic period across trials. Using repeated measures ANOVA, we asked if there was a significant main effect of error magnitude for errors in the CS-on direction (positive errors) for all errors larger than 0.5° (noting that as error magnitudes approach 0°, their direction is undefined). Our analysis suggested that there was not a significant relationship between probability of CS and error magnitude in the CS-on direction ($F_{10,530}=1.42$; $P=0.17$). Thus, once error direction was accounted for, we found no evidence for the hypothesis that error magnitude modulated probability of CS.

Quantifying trial-to-trial changes in behavior and SSs. In Fig. 2a we quantified how the presence of a CS in the postsaccadic period on trial n affected the next saccade in the same direction ($n+m$). To answer this question, we identified all trials in which the error was within 45° of the P-cell's preferred error direction (CS-on). For each trial, we then found the next trial in the same direction with the same target amplitude. We ensured that there were no more than one intervening trial between the first identified trial (with an error in CS-on) and the next trial with the same direction/target amplitude. In our experiment, the direction of the target on each trial was chosen pseudorandomly, with the caveat that the target eccentricity was never greater than ±30° from straight ahead. Therefore, by allowing an intervening trial in the opposite direction, we dramatically increased the amount of data available to determine trial-to-trial changes. After identifying pairs of trials in the same direction, we divided the pairs into two groups: those that had a complex spike during the postsaccadic period on trial n (CS present) and those that lacked a complex spike during this period (CS absent). For these two groups of trials, we found the trial-to-trial change in the saccade velocity profile from the first to the second trial, and then projected this change onto the CS-on direction for the

neuron. That is, imagine that $\dot{\mathbf{x}}^{(n)}(t)$ is the two dimensional saccade velocity profile in trial n, and $\dot{\mathbf{x}}^{(n+m)}(t)$ is the velocity profile of the next saccade in the same direction as trial n, (where $m = \{1 \text{ or } 2\}$). We found the trial-to-trial change in the velocity profile as $\mathbf{b}_i^T(\dot{\mathbf{x}}_i^{(n+m)}(t) - \dot{\mathbf{x}}_i^{(n)}(t))$, where $\mathbf{b}_i$ is a unit vector in the direction of CS-on for the ith neuron (i.e., $\left[cos(\theta_i^{(\text{CS-on})}) \quad sin(\theta_i^{(\text{CS-on})})\right]^T$) and the superscript T indicates the transpose operator. Our results indicated that the presence of a CS in trial n biased the next movement in the CS-on direction of the P-cell that expressed that CS (Fig. 2d).

In Supplementary Fig. 3, we project the trial to trial change onto CS + 90°, such that $\mathbf{b}_i = \left[cos(\theta_i^{(\text{CS-on})} + \pi/2) \quad sin(\theta_i^{(\text{CS-on})} + \pi/2)\right]^T$, whereas in Supplementary Fig. 4 we define $\mathbf{b}_i = \left[cos(\theta_i^{(\text{SS-on})}) \quad sin(\theta_i^{(\text{SS-on})})\right]^T$ and $\mathbf{b}_i = \left[cos(\theta_i^{(\text{SS-on})} + \pi/2) \quad sin(\theta_i^{(\text{SS-on})} + \pi/2)\right]^T$.

Identification of burst and pause cells. P-cells in the oculomotor vermis displayed heterogeneity in their responses during saccades (Supplementary Fig. 5). Some P-cells increased their activity (bursters), while others decreased their activity (pausers), or showed combinations of these responses. To demonstrate this diversity, we artificially divided our population of cells into two speculative classes: bursters and pausers. For each cell, we measured the average firing rate over the duration of each saccade to a target regardless of amplitude or direction. Cells that, on average, increased their activity relative to a baseline period (baseline defined as 200–50 ms before saccade onset) were classified as putative bursters, and all other cells were classified as pausers[4]. In our dataset, we identified $n = 35$ bursting cells and $n = 32$ pausing cells. The average responses of each of these two cell groups are shown in Fig. 3a. Both the burst and pause subpopulations showed saccade-related activity, but this activity was not directly related to real-time motion of the eye[4].

Population response. Approximately 50 P-cells in the cerebellar cortex project to a single neuron in the deep cerebellar nucleus (DCN)[26]. To estimate the population response in Figs. 3a and 4, we randomly sampled populations of 50 P-cells with replacement. The population response for this subset of neurons was the sum of instantaneous firing rates, corresponding to the number of presynaptic spikes that would be observed by the postsynaptic neuron in the caudal fastigial nucleus (cFN), the most medial of the deep cerebellar nuclei. Since individual P-cell SS responses in OMV are heterogeneous[24,31] (for example, bursting or pausing), simply estimating the s.e.m. across individual neuron responses would significantly overestimate the variance of the response observed by a cFN neuron. Therefore, we estimated confidence intervals on the population response by performing this same analysis 50 times and showing the mean population response with 95% confidence intervals across these 50 bootstrapped samples. Therefore, the error bars in the population response in Figs. 3a and 4b are 95% confidence intervals across the bootstrapped samples.

Saccade adaptation. For the vast majority of cells ($n = 56$), we were able to estimate the P-cell's CS-on direction online[16,24]. We then performed blocks of trials in which the targets were presented along the CS-on axis. During saccades to targets in either the CS-on or CS-on + 180° directions, the target was displaced inwards, eliciting gain-down adaptation (Fig. 4a). For the remainder of the cells ($n = 11$)[25], we performed gain-down adaptation strictly in the horizontal axis. Even for these cells, we were able to determine the P-cell's CS-on direction offline and assign the closest horizontal direction as CS-on. We were able to stably record the P-cells for an average of 1,069 ± 89 (mean ± s.e.m.) trials during the adaptation period. To collapse across sessions with different numbers of adaptation trials, we normalized the adaptation period for each P-cell between [0, 1]. Here 0 corresponds to the beginning of adaptation and 1 corresponds to the end of adaptation.

Statistical analysis. Statistical analysis was completed using R. We used two-tailed t tests to compare means without a repeated measures component. Remaining tests were performed using repeated-measures ANOVA (RM-ANOVA). Data distributions were assumed to be normal and not formally tested unless otherwise stated.

Reporting Summary. Further information on experimental design is available in the Nature Research Reporting Summary linked to this article.

Data and code availability. The data and analysis code of the current study are available from the corresponding author upon reasonable request.

References

46. Fuchs, A. F. & Robinson, D. A. A method for measuring horizontal and vertical eye movement chronically in the monkey. *J. Appl. Physiol.* **21**, 1068–1070 (1966).
47. Stone, L. S. & Lisberger, S. G. Visual responses of Purkinje cells in the cerebellar flocculus during smooth-pursuit eye movements in monkeys. II. Complex spikes. *J. Neurophysiol.* **63**, 1262–1275 (1990).

nature research

Corresponding author(s): David J. Herzfeld

Reporting Summary

Nature Research wishes to improve the reproducibility of the work that we publish. This form provides structure for consistency and transparency in reporting. For further information on Nature Research policies, see Authors & Referees and the Editorial Policy Checklist.

Statistical parameters

When statistical analyses are reported, confirm that the following items are present in the relevant location (e.g. figure legend, table legend, main text, or Methods section).

n/a	Confirmed	
☐	☒	The exact sample size (*n*) for each experimental group/condition, given as a discrete number and unit of measurement
☐	☒	An indication of whether measurements were taken from distinct samples or whether the same sample was measured repeatedly
☐	☒	The statistical test(s) used AND whether they are one- or two-sided *Only common tests should be described solely by name; describe more complex techniques in the Methods section.*
☐	☒	A description of all covariates tested
☐	☒	A description of any assumptions or corrections, such as tests of normality and adjustment for multiple comparisons
☐	☒	A full description of the statistics including central tendency (e.g. means) or other basic estimates (e.g. regression coefficient) AND variation (e.g. standard deviation) or associated estimates of uncertainty (e.g. confidence intervals)
☐	☒	For null hypothesis testing, the test statistic (e.g. *F*, *t*, *r*) with confidence intervals, effect sizes, degrees of freedom and *P* value noted *Give P values as exact values whenever suitable.*
☒	☐	For Bayesian analysis, information on the choice of priors and Markov chain Monte Carlo settings
☒	☐	For hierarchical and complex designs, identification of the appropriate level for tests and full reporting of outcomes
☐	☒	Estimates of effect sizes (e.g. Cohen's *d*, Pearson's *r*), indicating how they were calculated
☐	☒	Clearly defined error bars *State explicitly what error bars represent (e.g. SD, SE, CI)*

Our web collection on statistics for biologists may be useful.

Software and code

Policy information about availability of computer code

Data collection	Neurophysiology and behavioral data were collected on a Power 1401 (CED). Stimuli and live data traces were provided to the experimenter by a custom Spike2 script. For additional data collection information, see Herzfeld et al. (2015), as noted in the Methods section.
Data analysis	Data was analyzed using custom code written in python. Statistical analysis was performed using R (3.4). Analysis code is available upon reasonable request to the corresponding author (noted in the Methods section).

For manuscripts utilizing custom algorithms or software that are central to the research but not yet described in published literature, software must be made available to editors/reviewers upon request. We strongly encourage code deposition in a community repository (e.g. GitHub). See the Nature Research guidelines for submitting code & software for further information.

Data

Policy information about availability of data

All manuscripts must include a data availability statement. This statement should provide the following information, where applicable:

- Accession codes, unique identifiers, or web links for publicly available datasets
- A list of figures that have associated raw data
- A description of any restrictions on data availability

The data are available from the corresponding author upon reasonable request.

Field-specific reporting

Please select the best fit for your research. If you are not sure, read the appropriate sections before making your selection.

☒ Life sciences ☐ Behavioural & social sciences

For a reference copy of the document with all sections, see nature.com/authors/policies/ReportingSummary-flat.pdf

Life sciences

Study design

All studies must disclose on these points even when the disclosure is negative.

Sample size	N=7 monkeys were used in this experiment (reported in the first paragraph of the results section as well as the methods). This number exceeds the conventional n=2 monkeys used for most other neurophysiology studies. The number of neurons analyzed in this study (n=67) dramatically exceeds the number of Purkinje cells with stable complex spikes reported in most other studies (n of approx. 30)
Data exclusions	Exclusion criteria are listed in the method section. We excluded Purkinje cells in which the recording was not stable. That is, cells for which we could not accurately detect complex spikes throughout the recording were excluded. Exclusion criteria for trials are also described in the methods section (<5% of all saccades).
Replication	Our study reproduces the population gain-field encoding first presented in Herzfeld et al. (2015), expanding this representation for two additional monkeys.
Randomization	Our animals were not separated into groups.
Blinding	Our animals were not separated into groups, therefore blinding was unnecessary.

Materials & experimental systems

Policy information about availability of materials

n/a	Involved in the study
☒	☐ Unique materials
☒	☐ Antibodies
☒	☐ Eukaryotic cell lines
☐	☒ Research animals
☒	☐ Human research participants

Research animals

Policy information about studies involving animals; ARRIVE guidelines recommended for reporting animal research

Animals/animal-derived materials	Our study involves n=7 macaca mulatta (all males). Weight and age ranges are provided in the methods section.

Method-specific reporting

n/a	Involved in the study
☒	☐ ChIP-seq
☒	☐ Flow cytometry
☒	☐ Magnetic resonance imaging